Science of the Total Environment 785 (2021) 147247

Contents lists available at ScienceDirect

Science of the Total Environment

journal homepage: www.elsevier.com/locate/scitotenv

Spatiotemporal variations in damages to cropland from agrometeorological disasters in mainland China during 1978–2018

Ximeng Xu [a], Qiuhong Tang [a,b,*]

[a] Key Laboratory of Water Cycle and Related Land Surface Processes, Institute of Geographic Sciences and Natural Resources Research, Chinese Academy of Sciences, Beijing, China
[b] University of Chinese Academy of Sciences (UCAS), Beijing, China

HIGHLIGHTS

- Drought was the most severe with largest covered area of 22.2 million ha every year during 1978–2018.
- More than 70% of the covered area was induced by drought and flood in most provincial districts.
- Hail disasters were prominent in Xinjiang with significant increasing trends.
- LTF covered and affected the smallest cropland area but with an increasing trend.

GRAPHICAL ABSTRACT

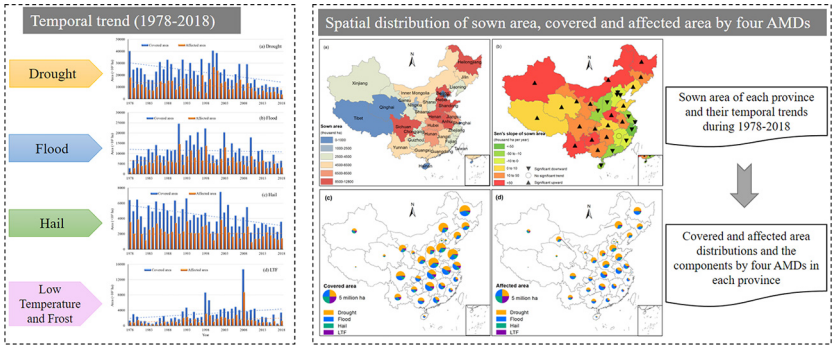

ARTICLE INFO

Article history:
Received 29 December 2020
Received in revised form 14 April 2021
Accepted 15 April 2021
Available online 21 April 2021

Editor: Jay Gan

Keywords:
Meteorological disasters
Cropland
Drought
Flood
Hail
Low temperature and frost

ABSTRACT

Drought, flood, hail, low temperature, and frost (LTF) are the main agrometeorological disasters (AMDs) in China; however, comprehensive and quantitative studies on cropland damage induced by AMDs across the whole country in terms of long-term trends are still lacking and urgently needed. Based on historical statistical data from yearbooks and bulletins, the overall characteristics of cropland damage by AMDs during 1978–2018 were analyzed using a pre-whitening procedure and a Mann-Kendall trend test at yearly and provincial scales in China. The results showed that drought was the most severe, with an average covered area of 22.2 million ha and an affected area of 11.2 million ha every year during 1978–2018, followed by flood, hail, and LTF. A decreasing trend was observed in covered area and affected area by drought, flood, and hail, while only LTF showed an increasing trend. On provincial scale, more than 70% of the covered area by AMDs was induced by drought and flood in most provincial districts. In all provincial districts of northern China, more than 50% of the covered area was induced by drought. In most provincial districts of southern China, more than 40% of the covered area was induced by flood. Hail disasters were prominent in Xinjiang, with significant increasing trends among all parameters. Compared with the other three AMDs, LTF covered and affected the smallest cropland area, but significant increasing trends were observed in the northwest and middle parts of China. The results of this study systematically display the characteristics of damage to cropland by four main AMDs, which are critical and necessary for disaster risk reduction and adaptive strategy development.

© 2021 Elsevier B.V. All rights reserved.

1. Introduction

Meteorological conditions are one of the most important factors influencing agriculture worldwide. Agriculture is particularly vulnerable to meteorological disasters as it is heavily reliant on weather,

* Corresponding author at: Key Laboratory of Water Cycle and Related Land Surface Processes, Institute of Geographic Sciences and Natural Resources Research, Chinese Academy of Sciences, Beijing, China.
E-mail address: tangqh@igsnrr.ac.cn (Q. Tang).

https://doi.org/10.1016/j.scitotenv.2021.147247
0048-9697/© 2021 Elsevier B.V. All rights reserved.

climate, land, and water (Food and Agriculture Organization of the United Nations, 2018). Agrometeorological disasters (AMDs) such as continuous drought, severe flood, hail by strong convective systems, and low temperature and frost (LTF) can significantly change the essential crop growth conditions, thereby reducing grain production over a large spatial range (Yao et al., 2017; Xu et al., 2017). World Meteorological Organization Statement on the State of the Global Climate (World Meteorological Organization, 2020) concluded that food security continues to be adversely affected by climate variability and extreme weather. Increasing temperatures and changing rainfall patterns have significantly changed terrestrial ecosystems, including agricultural lands and crop yields (Intergovernmental Panel on Climate Change, 2019). In accordance with the estimation of Food and Agriculture Organization of the United Nations (2018), agriculture (crops, livestock, forestry, fisheries and aquaculture) in developing countries experienced 26% of the total loss and damage incurred during medium- and large-scale climate-related disasters between 2006 and 2016. Approximately two-thirds of the damage to crops was associated with floods, and almost 90% of the damage to the livestock sector was attributable to drought. With the exception of agricultural losses, these disasters can also induce significant population effects and severe economic losses worldwide (Crompton and John McAneney, 2008; Guan et al., 2015; Wu et al., 2014; Liu and Yan, 2011; Zhou et al., 2014; Klomp, 2016; Tang et al., 2019).

In the past decades, the characteristics of extreme weather events have changed with respect to their frequency, magnitude, duration, and spatial range because of an increasingly extreme weather under climate change (Intergovernmental Panel on Climate Change, 2012; Sisco et al., 2017; Roxburgh et al., 2019; Tang, 2020). The rising incidence of weather extremes will have increasingly negative impacts on agriculture because critical thresholds are already being exceeded, thus creating an increasing trend of AMDs worldwide (Alcántara-Ayala, 2002; Piao et al., 2010; Konisky et al., 2016; Stott, 2016; Wang et al., 2017). Such increased AMDs can reduce cropland production, causing direct economic losses to farmers and affecting rural livelihoods (Jin et al., 2016; Yan et al., 2017; Parisse et al., 2020). Moreover, these increased AMDs will also have long-lasting and multi-pronged consequences such as loss of harvest and livestock, disease outbreaks, and destruction of rural infrastructure and irrigation systems (Wu et al., 2015; Qiu et al., 2018; Li et al., 2018; Ye et al., 2020). Thus, there is an urgent need to better understand the characteristics of AMDs and their damage to cropland for their adaptive management.

China is one of the countries experiencing the most sever AMDs worldwide because of its monsoon climate conditions and dense disaster-bearing bodies (Zhang et al., 2014a,b). The damage induced by metrological disasters can account for more than 70% of all natural disasters (Qin, 2007; Shi and Ying, 2016). Every year, more than 50 million hectares of agricultural land are affected by AMDs, which has been the main barrier for stable grain production (Zhang et al., 2014a,b; Huang et al., 2017; Wang et al., 2017). During the past decades, a number of studies have concentrated on AMDs in China. Wang et al. (2006) comprehensively analyzed the characteristics of natural disasters in China, including spatial distributions, temporal dynamic processes and impacts on social economy. More detailed studies have been conducted on different aspects of meteorological disasters, such as hazard-causing environments (Yin et al., 2009; Su et al., 2011), risk assessment (Zhang, 2004; Hao et al., 2012; He et al., 2013; Zhou et al., 2015), temporal and spatial distribution characteristics (Fang et al., 2011; Zhang et al., 2014b; Guan et al., 2015; Fu et al., 2018; Wang et al., 2019a), and disaster impact assessments (Liu and Yan, 2011; Huang et al., 2019; Guo et al., 2020). Recently, the impact of meteorological disasters on agriculture has been summarized and analyzed (Hao et al., 2012; Zhang et al., 2014a,b; Fu et al., 2018; Wang et al., 2019a; Liu et al., 2019; Huang et al., 2019; Guo et al., 2019). However, their results are limited without comprehensive summaries on the spatiotemporal characteristics of cropland damage caused by AMDs in China. Most of these studies have been conducted at regional scales (Wang et al., 2017; Xu et al., 2017; Huang et al., 2017; Fu et al., 2018; Liu et al., 2019; Huang et al., 2019). There have also been some nationwide and provincial-level studies on single crops (Zhang et al., 2014a,b; Huang et al., 2019) by single or limited types of AMDs (Fang et al., 2011; Liu and Yan, 2011; Hao et al., 2012; He et al., 2016; Yao et al., 2017; Liu et al., 2019; Chou et al., 2019; Wang et al., 2019a; Guo et al., 2020). Although previous studies provide a detailed understanding of specific crops and disasters, comprehensive and quantitative studies on the impact of AMDs on cropland losses over entire country in long-term trends are still lacking and urgently needed.

The main objective of this study is, therefore, to display the spatiotemporal variations in damage to cropland by four different AMDs in mainland China during 1978–2018. The results can provide a scientific basis for studies on AMDs, and help decision-makers and local governments adjust their adaptive strategies. Adaptive measures can help mitigate the impact of AMDs and improve food security and poverty prevention in China.

2. Data and methodology

2.1. Data

Historical cropland damage data induced by different AMDs (including drought, flood, hail, and LTF) were used to display the spatiotemporal variations in the last four decades from 1978 to 2018 at both national and provincial scales. The covered and affected area data from drought and flood were collected from the Bulletin of Flood and Drought Disasters in China (The Ministry of Water Resources of the People's Republic of China, 2018) and the China Agricultural Statistical Report (The Ministry of Agriculture of the People's Republic of China, 2018). The covered and affected area data by hail and LTF were collected from China Agricultural Statistical Report. In these yearbooks and statistical reports, the covered area and affected area of cropland in each year for each provincial district were collected. Covered area was defined as the sown area with over 10% (including 10%) crop losses due to AMDs, while the affected area was defined as the sown area with over 30% (including 30%) crop losses due to AMDs (Table S1). These data were used to illustrate the long-term changing trends of cropland losses by AMDs during the past four decades. The cropland sown area of each province in each year was acquired from the Chinese Statistical Yearbook (National Bureau of Statistics of China, 2018). Then the covered percentage and affected percentage were calculated as covered area and affected area divided by cropland sown area for each provincial district in each year from 1978 to 2018. Table S1 summarizes the definitions of indexes used in this study.

There is a general county-prefecture-province three-level system for statistics and reporting processes of damage caused by different disasters. Disaster information reporting procedures are divided into initial reports, renewal reports, and verification reports. There are also some quality control processes after the central government receives a report. Thus, the disaster data quality used in this study is convincing and comprehensive, with no data gaps. They are quality controlled by the statistical organization at the national level and an on-site inspection by local and central governments. In this study, cropland damage by four types of AMDs (drought, flood, hail, and LTF) was included. During the statistical processes of cropland damage caused by drought, the damage information was continuously updated for a single agricultural drought event. Thus, a drought event was counted when cropland damage data were no longer reported and updated by the three-level disaster reporting system, and the total cropland damage was recorded. Then, the cropland damages induced by all events in one year were added together and included in the annual cropland damage data series. Cropland damage data for other AMDs were also calculated using the same method. Flood disasters include the disasters induced by an increase in water volume of rivers, lakes, and coastal areas, the flooding of

water levels, and the outbreak of mountain torrents as a result of heavy rainfall, melting of ice and snow, ice slush, dike breach, storm surge, etc. Hail disasters refer to disasters caused by strong winds, hail, tornadoes, and lightning caused by a strongly convective weather. LTF disasters include low-temperature continuous rain, low-temperature cold damage, frost, and cold waves. Snowstorm disaster was merged with LTF disaster as they were always accounted together. Overlapping effects of different AMDs occurring in the same area for one year were also considered: when the crops in the same area suffered more than one disaster event, only the severest one was counted (Table S1).

For the spatial distribution, it should be noted that Taiwan province, Hong Kong and Macao were not included in the analysis because of incomplete data. Hainan province was separated from Guangdong province in 1988, and Chongqing municipality was separated from Sichuan province in 1997. Thus, the data of Hainan province and Chongqing municipality were collected from 1988 and 1997 onward, respectively. When conducting the trend analysis, the values of Hainan province and Guangdong province were added as one value, and the values of Chongqing municipality and Sichuan province were also added, to ensure the consistency of the data collection area. Thus, the changing trends in Hainan, Guangdong, Chongqing and Sichuan have the same value.

2.2. Methodology

The non-parametric Mann-Kendall test was applied to detect time series trends of indexes from 1978 to 2018 (Mann, 1945; Kendall, 1975). This method is suitable for data that do not follow a normal distribution, and are less sensitive to outliers. It has been widely used and recommended by the World Meteorological Organization as a standard procedure for examining trends in hydro-meteorological data that are serially independent (Hamed and Ramachandra, 1998; Tabari and Talaee, 2011; Song et al., 2015; Dawood, 2017; Shiru et al., 2019).

The null hypothesis H_o is that the dataset X_t (x_1, …, x_n) of a generic variable is independent and identically distributed. The alternative hypothesis H_1 is that a monotonic trend exists in the dataset. Then, the Z value is used to judge the direction of the trend and is calculated by using the following formula:

$$Z = \begin{cases} \dfrac{S-1}{\sqrt{Var(S)}} & S > 0 \\ 0 & S = 0 \\ \dfrac{S+1}{\sqrt{Var(S)}} & S > 0 \end{cases}, \tag{1}$$

The test static S is calculated using Eqs. (2) and (3), while the variance is computed using Eq. (4).

$$S = \sum_{k=1}^{n-1} \sum_{j=k+1}^{n} sgn\,(x_j - x_k), \tag{2}$$

$$sgn\,(x_j - x_k) = \begin{cases} 1 & if\,(x_j - x_k) > 0 \\ 0 & if\,(x_j - x_k) = 0 \\ -1 & if\,(x_j - x_k) < 0 \end{cases}, \tag{3}$$

$$Var(S) = \frac{\left[n(n-1)(2n+5) - \sum_{i=1}^{m} t_i(t_i-1)(2t_i+5)\right]}{18}, \tag{4}$$

where the distributions of x_k and x_j are not identical for all $k, j \le n$ with $k \ne j$, $n \ge 10$ is the length of the dataset, m is the number of tied groups (a tied group is a set of sample data having the same value), and t_i is the number of data points in the i-th group. If $|Z| \ge Z_{1-\alpha/2}$, then the null hypothesis is rejected, and a significant trend exists in the series at the set level of α. Positive values of Z indicate upward trends, whereas negative values of Z show downward trends. The greater the absolute value of Z, the more significant the trend of the sequence. In this study, a significance level of $\alpha = 0.05$ was applied.

A portion of the cropland damage data series included in this study exist the serial correlation of time series. To eliminate the influence of serial correlation on the Mann-Kendall test, a pre-whitening method was applied in this study. This method was first suggested by Von Storch (1995) and was further applied to detect trends in hydrological series (Yue et al., 2002; Yue and Wang, 2002). The pre-whitening process was conducted using the following equation:

$$Y_t = X_t - r_1 X_{t-1}, \tag{5}$$

where Y_t is the new dataset without the serial correlation of time series, which is applied in the Mann-Kendall test, and r_1 is the lag 1 serial correlation coefficient of data.

Sen's slope (Sen, 1968) was used to estimate the cover and affected area changes per year using four AMDs. The slope was estimated using Eq. (6) as follows:

$$SL = \text{Median}\left(\frac{x_j - x_k}{j-k}\right), \tag{6}$$

where SL is the estimate of the slope of the trend.

3. Results and discussion

3.1. Temporal changes of cropland covered and affected by AMDs at country scale

The temporal variations of areas covered and affected by drought, flood, hail, and LTF across the whole country during 1978–2018 are shown in Fig. 1.

Cropland areas covered and affected by drought have generally decreased over the last four decades (Fig. 1a). The average covered area and affected area by drought are 22.2 million and 11.2 million ha, respectively. The covered area and affected area of drought both show significant decreasing trends with slopes of −428.6 and −160.8 thousand ha per year, respectively ($p < 0.05$). The average covered area and affected area by flood are 11.4 million and 6.2 million ha, respectively, and they decrease at a rate of −41.7 and −20.3 thousand ha per year without any significant trend (Fig. 1b).

The cropland area covered and affected by hail and LTF showed opposite trends. From 1978 to 2018, the average covered area and affected area by hail are 4.4 million and 2.3 million ha, respectively (Fig. 1c). The cropland area covered and affected by hail significantly decreased from 1978 to 2018 with slopes of −70.9 and −31.0 thousand ha per year ($p < 0.05$), respectively. The average covered area and affected area by LTF are 3.1 million and 1.4 million ha, respectively (Fig. 1d), and they both show significant increasing trends with slopes of 55.9 and 16.0 thousand ha per year ($p < 0.05$), respectively. In 2008, a severe LTF disaster hit the south part of China (Hui, 2009), which induced 14.7 million and 8.7 million ha of cropland covered and affected by the LTF, respectively.

3.2. Spatiotemporal variations of sown area on provincial scale

The cropland area covered and affected by AMDs are not only related to natural phenomena, but also to the total sown area. The spatial distribution and temporal trends of the sown area of each provincial district during 1978–2018 are shown in Fig. 2. In the last four decades, Henan province has shown the largest mean annual sown area of 12.78 million ha, with a significant increasing slope of 103 thousand ha per year. Large sown areas of over 8.5 million ha are also found in Shandong, Heilongjiang, Sichuan, Hebei, and Anhui provinces, all of which have a high grain production. Qinghai and Tibet provincial districts have large territorial areas but small sown areas of less than one million ha because of poor planting and crop growing conditions on the Tibetan Plateau. The changing trends of sown area were significant in most provincial

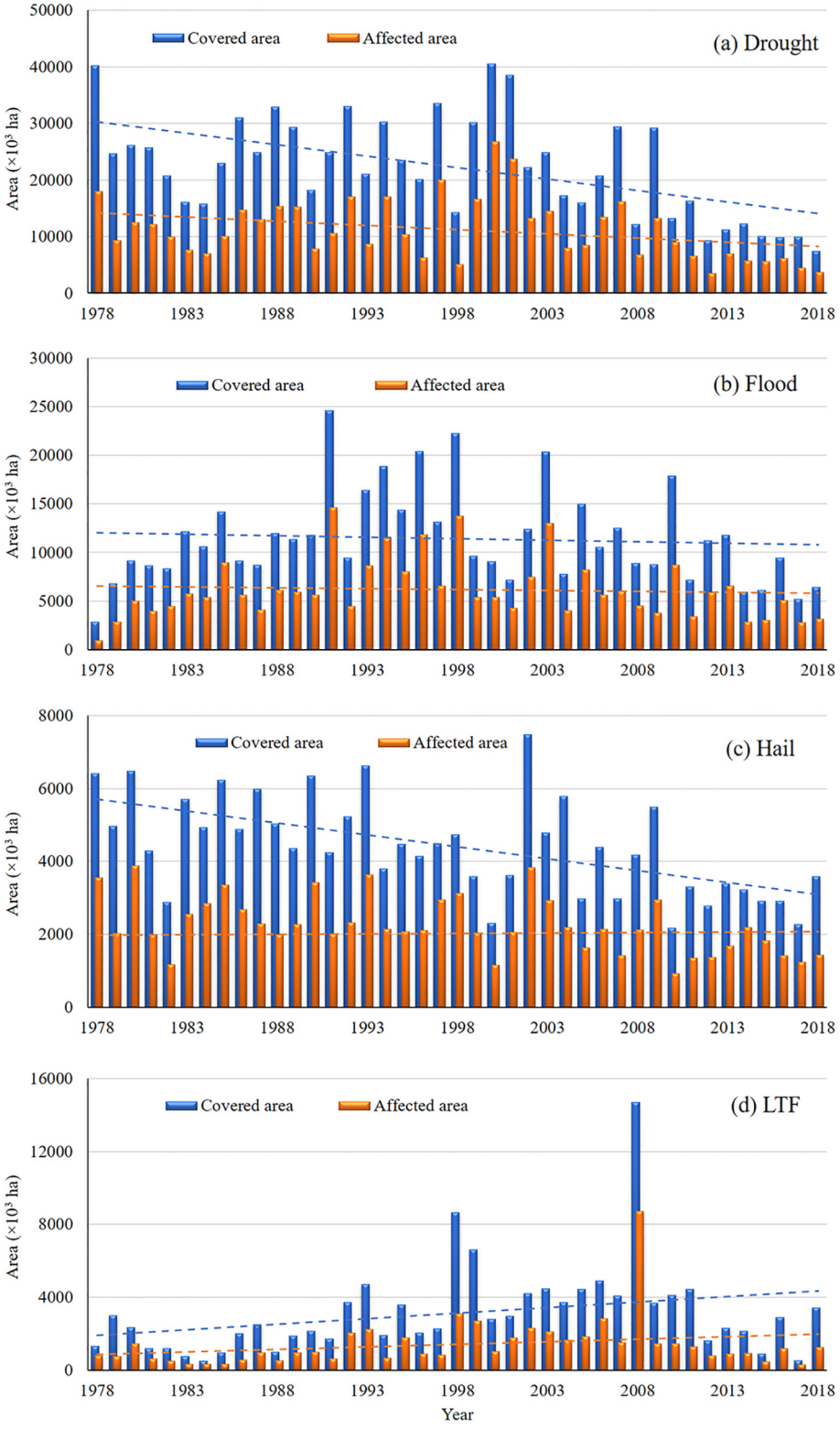

Fig. 1. Temporal variations of cropland areas covered and affected by drought (a), flood (b), hail (c), and LTF (d) of mainland China. Dashed lines represent the trends of covered and affected areas by four AMDs.

districts during 1978–2018 and correlated with economic development and government policy. Southeastern coastline provinces, such as Jiangsu, Zhejiang, Fujian, and Guangdong, showed significant downward trends because of rapid economic development, with the largest downward slope displayed in Zhejiang province. Shanxi and Shaanxi provinces also showed downward trends that might have been caused by the Grain for Green Project implemented in 1999 (Feng et al., 2005; Chen et al., 2015). Among the four municipalities directly under the central government, the sown areas of Beijing, Tianjin, and Shanghai showed a significant decreasing trend as these cities rapidly expanded during 1978–2018. The sown areas of Jiangxi, Hebei, and Hainan provinces showed a slight decrease with no significant trend. Except for

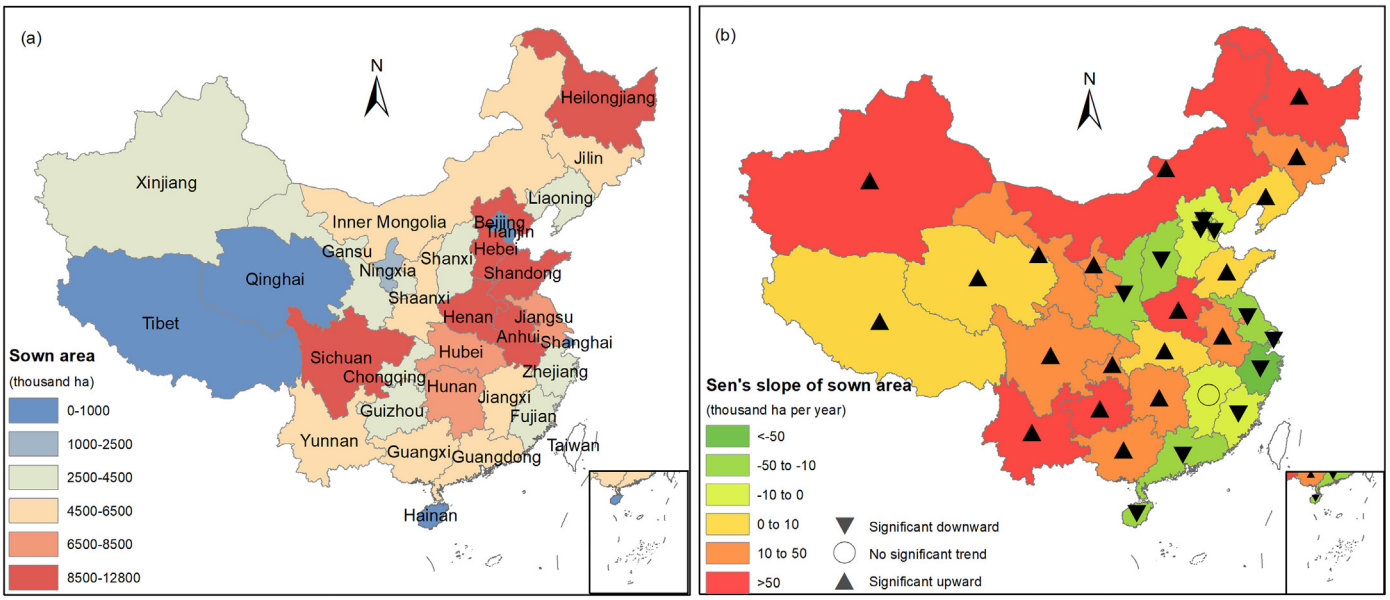

Fig. 2. The mean annual sown area on provincial scale (a) and changing trends from 1978 to 2018 (b). The provincial names are labeled in panel (a).

the provincial districts mentioned above, other provincial districts showed significant increasing trends, with slopes ranging from 1.2 to 115.7 thousand ha per year. Among them, Heilongjiang, Henan, Inner Mongolia, and Yunnan showed the highest increasing slopes of approximately 100 thousand ha per year.

3.3. Spatial distribution of covered and affected percentages by the four different AMDs

The summation of covered and affected percentages by the four AMDs and their component parts is shown in Fig. 3. The total covered and affected percentages are relatively higher in northern provincial districts than in the provinces of South China (Fig. 3a, b), indicating that croplands in these provinces have higher chance of being covered or affected by the AMDs, that is, they are vulnerable to AMDs induced by harsh natural conditions. It can also be concluded that the covered percentage and covered area are different among provincial districts (Fig. 3a, c), because the total sown area of each individual province is different (Fig. 2), and also because the natural climate conditions and disaster proofing ability of each province are different. In northwest China, such as Qinghai province, the covered percentage is higher than 35%, but the total cover area is approximately only 0.2 million ha because of a small sown area, where the natural conditions are not suitable for agriculture; similar conditions are observed in Tibet, Xinjiang. The total covered areas by AMDs are the highest at around 3.0 million ha in the provinces with large sown areas, such as Heilongjiang, Henan, and Shandong (Fig. 3c).

The components of the four AMDs varied among different provincial districts (Fig. 3c). In most provincial districts, drought and flood were the two main AMDs, comprising more than 70% of the covered area during 1978–2018. In all provincial districts of northern China, more than 50% of the covered area was induced by drought, and this percentage reached approximately 75% in province such as Shanxi. The spatial distributions of cropland damage by drought were influenced by the precipitation and temperature distribution patterns. Among the four AMDs, drought covered and affected a larger percentage of croplands in northern China, suggesting it to be highly vulnerable to drought. This was also observed in other countries with similar climate zones such as Nigeria (Shiru et al., 2019). It should be noted that cropland damage induced by drought phenomenon is not only typically associated with the actual severity of the natural phenomenon; other factors such as applied agricultural practices (e.g., irrigation) can significantly reverse the disadvantages of drought. An improvement in drought proofing may have also contributed to the general decrease in cropland damage by drought over the last four decades, as displayed in Fig. 1a. In the southern part of China, floods occupied more than 40% of the covered areas in most provincial districts. The spatial distribution characteristics of cropland damage caused by floods corresponded well to the spatial distribution of precipitation and water resources because the southern part receives a larger amount of precipitation during long wet seasons (Wang and Zhou, 2005; You et al., 2011).

The affected percentage and affected area (Fig. 3b, d) displayed similar spatial trends as the cover area and covered percentage at a provincial scale. The largest affected area can be found in Heilongjiang and Inner Mongolia with more than 1.5 million ha, followed by the provinces located on the North China Plain and South-Central China with large sown areas.

3.4. Temporal changes of cropland area covered and affected by four different AMDs

The covered area and its temporal change slope are displayed to show the combined impact of changes in sown area and the probability of being covered by AMDs. The covered percentage and its temporal change slope are also displayed to show the impact of changes in the probability of being covered by AMDs, by eliminating the influence of the sown area. The same comparisons are also made with the affected area and affected percentage by the four AMDs.

3.4.1. Drought

Agricultural drought is one of the most frequent and widespread AMDs in China and significantly influences the crop yield and production (Zhang et al., 2014a; Yang et al., 2020; Shi et al., 2021). During 1978–2018, the covered area by drought in Inner Mongolia, Heilongjiang, Hebei, Shanxi, and Henan exceeded 1.2 million ha (Fig. 4a). Among them, Inner Mongolia shows the only significant increasing trend with a rate of 31.4 thousand ha per year throughout all provincial districts (Fig. 4b). This result fits well with the drought variation results obtained by Wang et al. (2019b) in Inner Mongolia, where the central and eastern regions of the study area showed a drought tendency. The spatial distribution of covered percentage indicates that cropland in the northern part of China has a higher probability of being covered

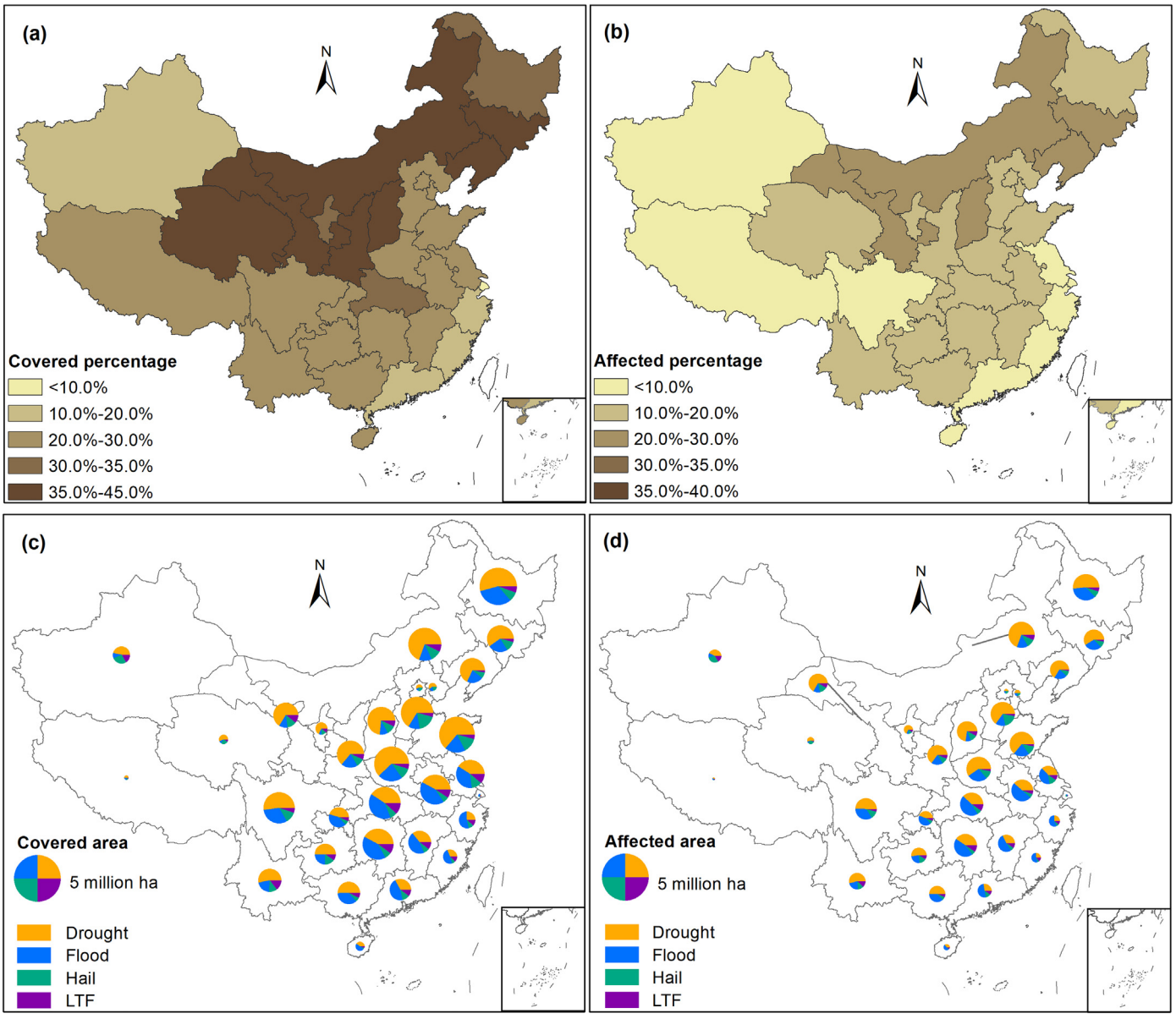

Fig. 3. Spatial distribution of total covered percentage (a), total affected percentage (b), components of covered area (c), and components of affected area (d) by four AMDs.

by drought than the southern part (Fig. 4c). The covered percentages of Inner Mongolia, Qinghai, Gansu, Shaanxi, Shanxi, Jilin, and Liaoning are all higher than 20%, which is the most severe among the four AMDs. As for the trend slopes of covered percentage (Fig. 4d), except for Inner Mongolia, Qinghai, and Gansu, which showed a non-significant increasing trend, all others showed a downward trend. This indicates the probability of being covered by drought has decreased in most parts of China. This probability of being covered by drought is not only related to the natural phenomenon of agricultural drought with unusual and significant soil or vegetation water deficiencies, but also to social and human factors. Other studies indicated a decrease in meteorological drought in most parts of China, except for the Mongolian Plateau and Yunnan-Guizhou Plateau (Zhou et al., 2017). At the same time, a better allocation of agricultural drought prevention and mitigation measures has also contributed to this decrease (Wu et al., 2020). Among these social and human factors, better agricultural infrastructure construction can significantly enhance the drought disaster combating ability. Moreover, the differences in crop species and applied agricultural practices can also lead to the variations in cropland damage. Crop species with better drought resistance ability and irrigation practices can significantly help a cropland mitigate a drought risk. The contributions of these factors to cropland damage variations require further detailed studies.

Compared with the spatial distribution of covered area and percentage, similar conditions can also be found in affected area and percentages, as well as their temporal trends (Fig. S1). For the affected area, Inner Mongolia and Xinjiang showed a significant increasing trend, while the affected percentage showed no significant trend. This implies the increasing affected area in Inner Mongolia and Xinjiang is primarily because of an increase in sown area.

For future drought disaster characteristic prediction, Yao et al. (2020) used multiple GCMs to identify the future drought characteristics in China and concluded that drought conditions would worsen because of increased minimum and maximum air temperatures although the annual precipitation increase was projected in most regions. In some high-interest regions such as the Yangtze River basin, the duration of drought was anticipated to increase in the future, especially for agricultural drought, and the headwater areas were anticipated to increase in agricultural drought severity (Sun et al., 2019). These results call for more reasonable and precise drought adaptation strategies in different regions when facing future climate changes.

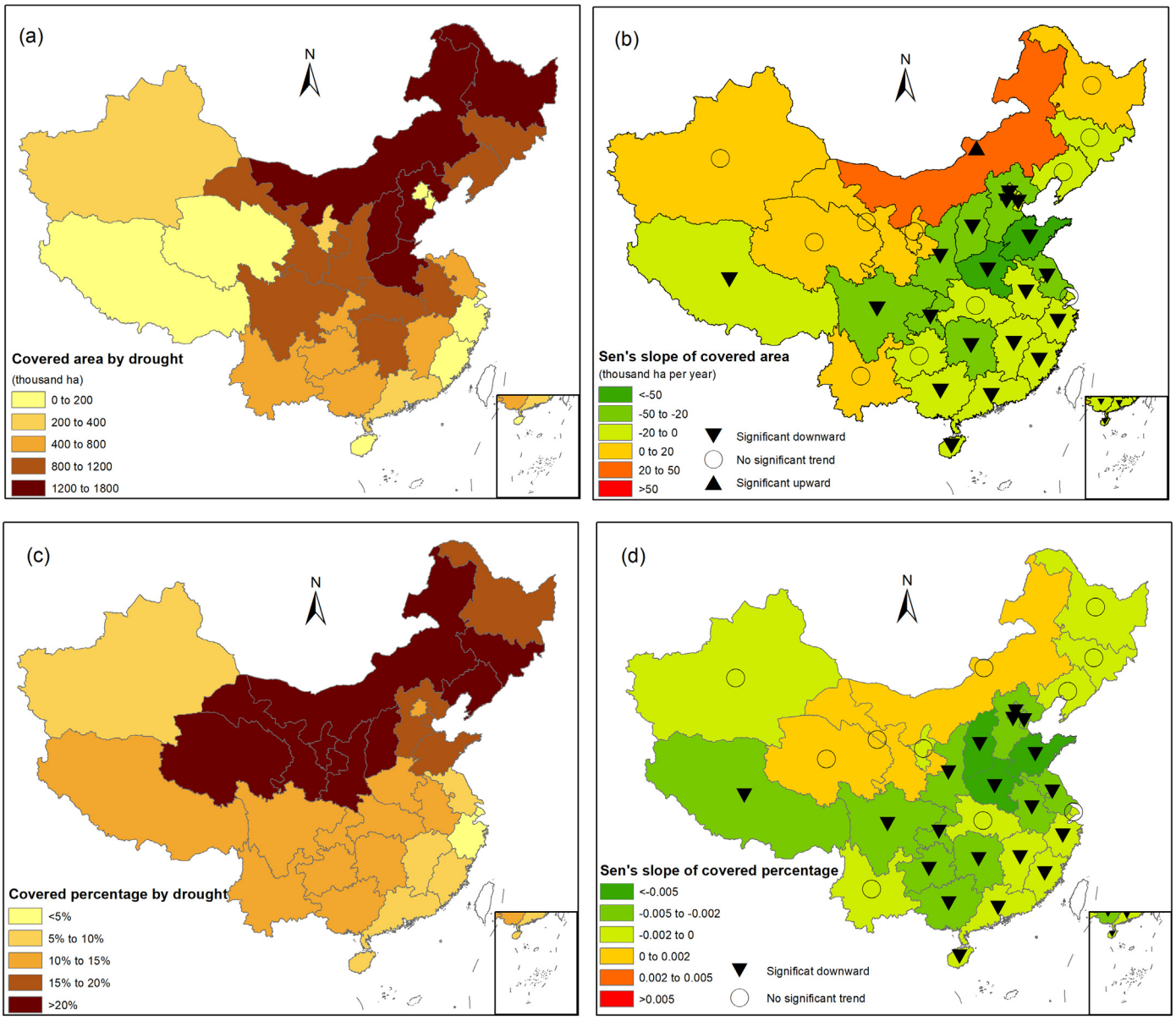

Fig. 4. Spatial distribution of covered area (a), covered percentage (c) and corresponding temporal change slope (b, d) from 1978 to 2018 by drought.

3.4.2. Flood

Flood disaster also plays an important role in reducing agricultural production in many parts of China (Zhang et al., 2014a,b; Guo et al., 2019). Cropland damage induced by flood disasters is mainly distributed in the middle to lower reaches of the Yangtze River basin, Songhua River basin, and Peral River basin (Fig. 5). Covered area by flood in Heilongjiang, Hubei, Hunan, and Anhui provinces are more than 0.7 million ha (Fig. 5a). Covered percentages larger than 10% are also observed in these provinces, as well as in Chongqing, which are all located in the Yangtze River basin and Songhua River basin (Fig. 5c). Studies on flood disaster risk assessment, disaster impact, and adaptation strategies have also been conducted in these regions for sustainable flood disaster management (Su et al., 2011; Liu et al., 2019; Gong et al., 2019; Wu et al., 2019). As for the trends of covered area and covered percentage, Xinjiang, Tibet, and Guangxi show significant increasing trends, while Hubei, Jiangxi and Hunan show non-significant increasing trends (Fig. 5b, d). These results illustrate that more anti-flood agricultural measures should be implemented to mitigate the possible influence of floods on croplands in these provincial districts.

For affected area by flood, Hubei, Hunan, Anhui and Heilongjiang provinces also show larger values of more than 0.5 million ha (Fig. S2a), while for affected percentage, Chongqing, Hubei, Hunan, Anhui, and Jiangxi show more than 6% (Fig. S2c). According to the trend analysis results from 1978 to 2018, the affected area by flood in many southern provincial districts show significant upward trends including Yunnan, Guizhou, Guangxi, Hubei, Hunan, and Jiangxi (Fig. S2b), which corresponds well with the results reported by Liu et al. (2019). The affected percentage by flood in Hubei, Hunan, and Jiangxi show significant increasing trends (Fig. S2d), demonstrating the increased probability of being affected by severe flooding of croplands in the middle reach of the Yangtze River basin. The same situations can also be observed in Xinjiang, Tibet and Qinghai. In coastal provinces such as Zhejiang, the covered/affected area decreases, whereas the covered percentage increases, suggesting that the decrease in sown areas has contributed to the decrease in the covered/affected area. Even when agricultural hazard-bearing bodies are decreasing, the coastal flood risk in China is expected to increase in the future (Fang et al., 2020), necessitating appropriate strategies to adapt to an

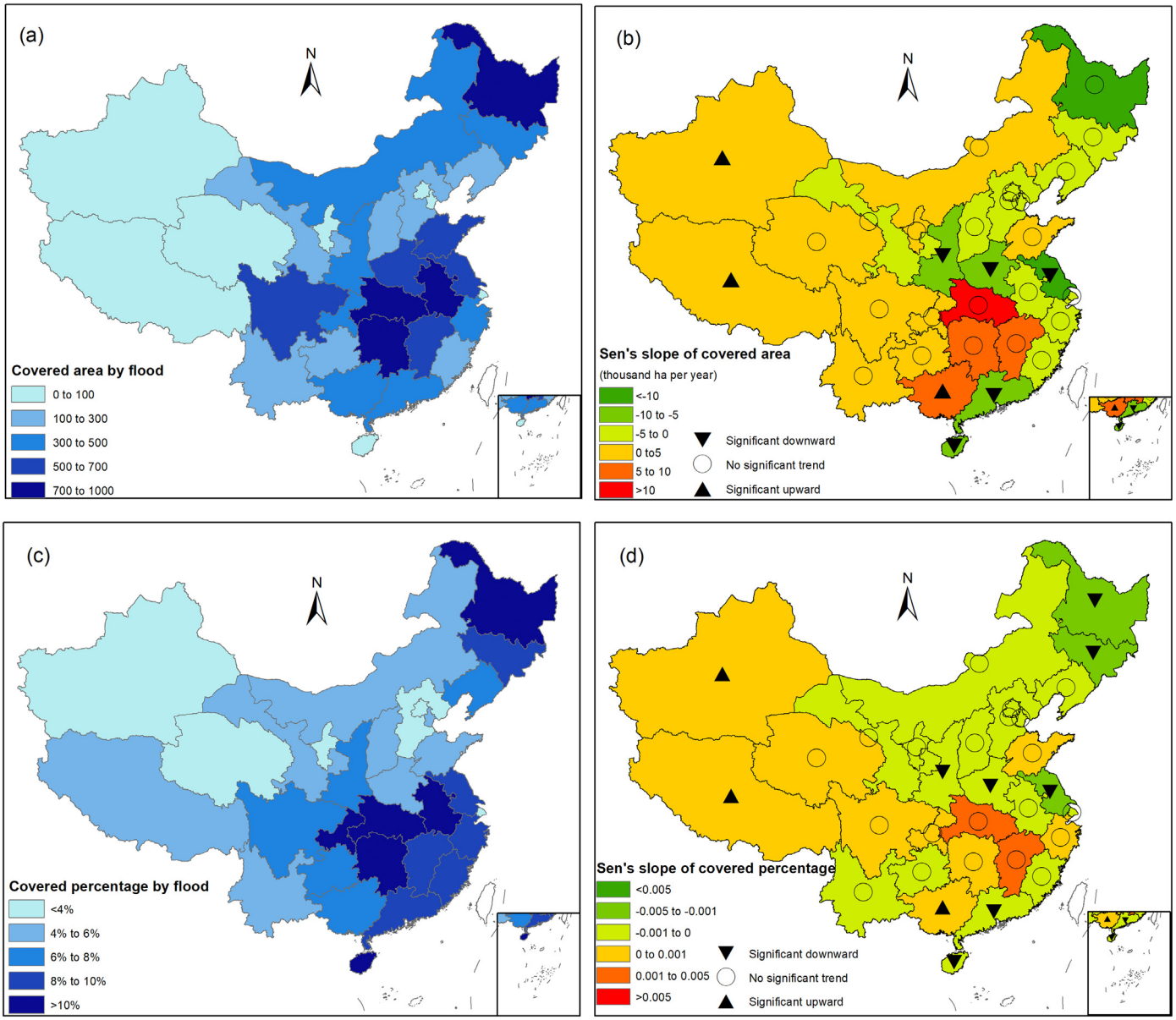

Fig. 5. Spatial distribution of covered area (a), covered percentage (c), and corresponding temporal change slope (b, d) from 1978 to 2018 by flood.

uncertain environment (Chen et al., 2020), and better deal with the relationship between agriculture and flood risk management (Kenyon et al., 2008).

3.4.3. Hail

The spatial distribution and trend analysis results of cropland damage caused by hail disasters during 1978–2018 are shown in Fig. 6. Compared with the absolute values of covered and affected areas by drought and flood, the values of hail disasters are relatively smaller. As for covered area and affected area, which are influenced by both sown area changes and the probability of being covered and affected by hail disaster, most northern provincial districts show higher values than southern provincial districts (Figs. 6a, S3a). In Hebei and Shandong, the covered area induced by hail disasters exceeds 0.3 million ha. As for covered percentage and affected percentage, Qinghai shows an extremely high covered percentage of more than 8% and affected percentage of more than 4% (Figs. 6c, S3c), demonstrating the largest probability of being covered and affected by hail disasters.

Trend analysis results show that a majority of provincial districts experienced downward trends during 1978–2018. Meanwhile, parameters including covered and affected areas as well as percentages by hail in Xinjiang all show significant increasing trends (Figs. 6b, d, S3b, d), which displays an increasing risk of hail disasters in Xinjiang. Shi et al. (2015) classified the severity of hail disasters and pointed out the high-risk region in Xinjiang, which provided some directional guidance for hail disaster mitigation. Extreme weather such as hailstorms is expected to increase under future climate change, thus, the mitigation measures should be better allocated according to risk assessment results to avoid severe agricultural and economic losses from hail disasters (Prein and Holland, 2018).

3.4.4. LTF

Compared with the other three AMDs, the lowest values of covered and affected area are observed with LTF (Figs. 7, S4). For covered area by LTF, southern provinces such as Hubei, Hunan, and Jiangsu have a covered area larger than 0.2 million ha, followed by provincial districts such as Yunnan, Gansu, Inner Mongolia, and Heilongjiang with a covered area larger than 0.15 million ha (Fig. 7a). This distribution is attributed to both sown area distribution and natural meteorological characteristics related to LTF disasters. Trend analysis results show

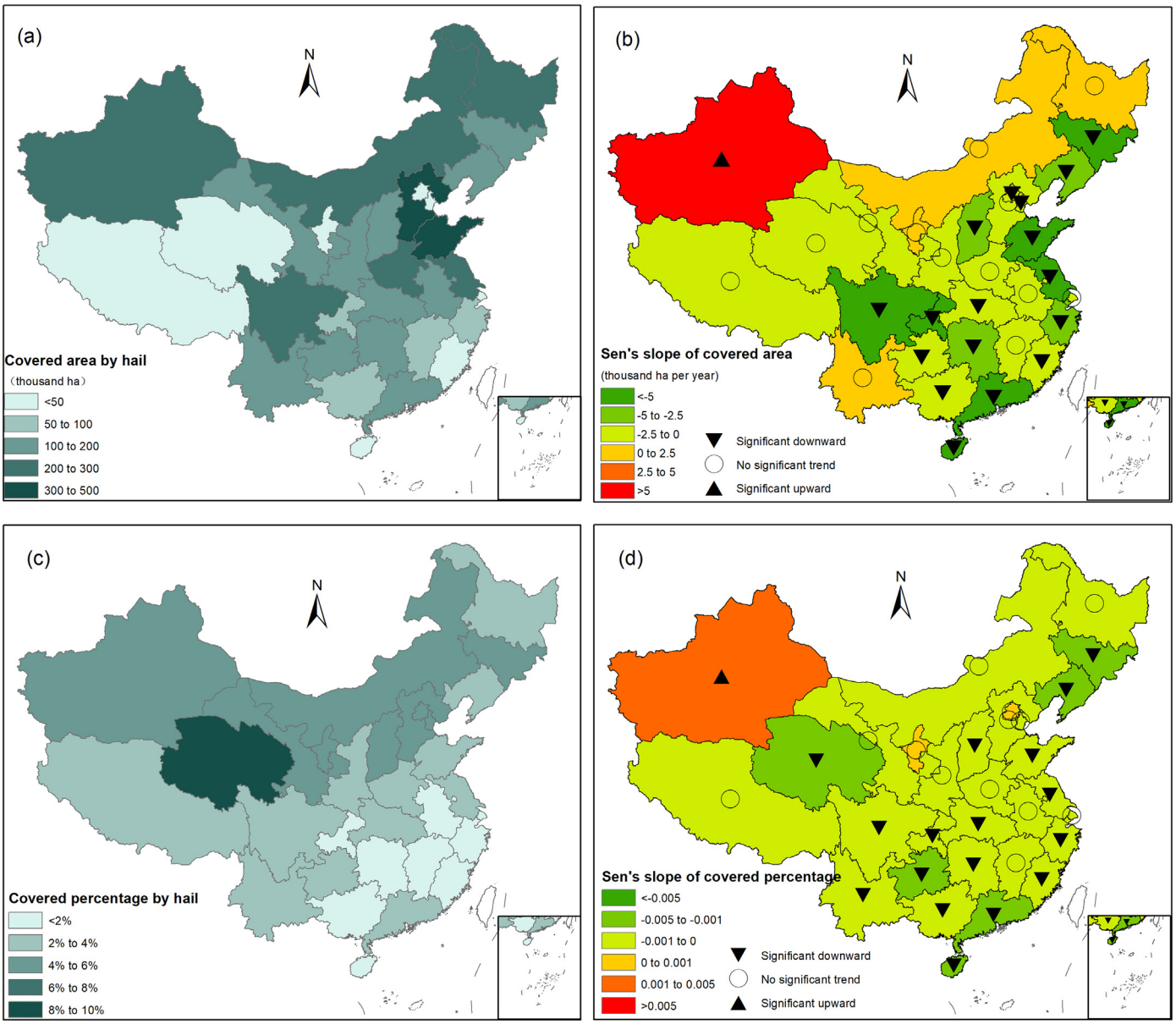

Fig. 6. Spatial distribution of covered area (a), covered percentage (c), and corresponding temporal change slope (b, d) from 1978 to 2018 by hail.

that the northwest, north and middle provincial districts have experienced significant upward trends, especially in Xinjiang, Gansu, Hubei, and Hunan; the increasing rates are all larger than 2 thousand ha per year (Fig. 7b). The covered percentage by LTF varies among different provinces; the largest percentage is observed in Gansu Province, which is more than 4% (Fig. 7c). The change rate distributions of the covered percentage are similar to those of the covered area (Fig. 7d), and the northwest and middle parts show significant increasing trends. These increasing trends can be explained by the increasing number of extreme cold weather conditions and more croplands with a higher vulnerability to LTF. Although the mean temperature increases under a global warming background, an extremely cold weather may occur more frequently in some regions (Tang et al., 2013; Kim and Lee, 2019).

The affected area by LTF in Hubei and Hunan provinces is the largest with more than 0.1 million ha (Fig. S4a); these two provinces also show a significant upward trend during 1978–2018 (Fig. S4b). Other provincial districts, such as Xinjiang Shanxi, Inner Mongolia, and Hebei, also show significant increasing trends. The affected percentage by LTF in all provincial districts is less than 2%, and the overall values in the northwest are larger than those in the southeast part (Fig. S4c). The trend analysis results show that the affected percentage of Xinjiang, Shanxi, Hebei, and Hunan significant increase, while Chongqing follows a decreasing trend (Fig. S4d). Owing to the special stepped topography and different climate zones of China, the LTF disaster shows a zonal differentiation; these distribution results correspond well with Gao (2016) and Su et al. (2011). The increased trend detected in the central and southern parts of China also confirm the result from Gao (2016) that high loss regions shifted from the northwest to the southeast with accelerated urbanization, rapid economic development, and facility cultivation. These results highlight the need to strengthen disaster prevention in central and southern China.

4. Concluding remarks

This study analyzed the spatiotemporal characteristics of cropland damage by four main AMDs (drought, flood, hail, and LTF) in mainland China in the last four decades, from 1978 to 2018. The results showed that the average covered area and affected area by drought were largest among four AMDs, with yearly averaged values of 22.2 million and 11.2 million ha per year from 1978 to 2018, followed by flood with values of

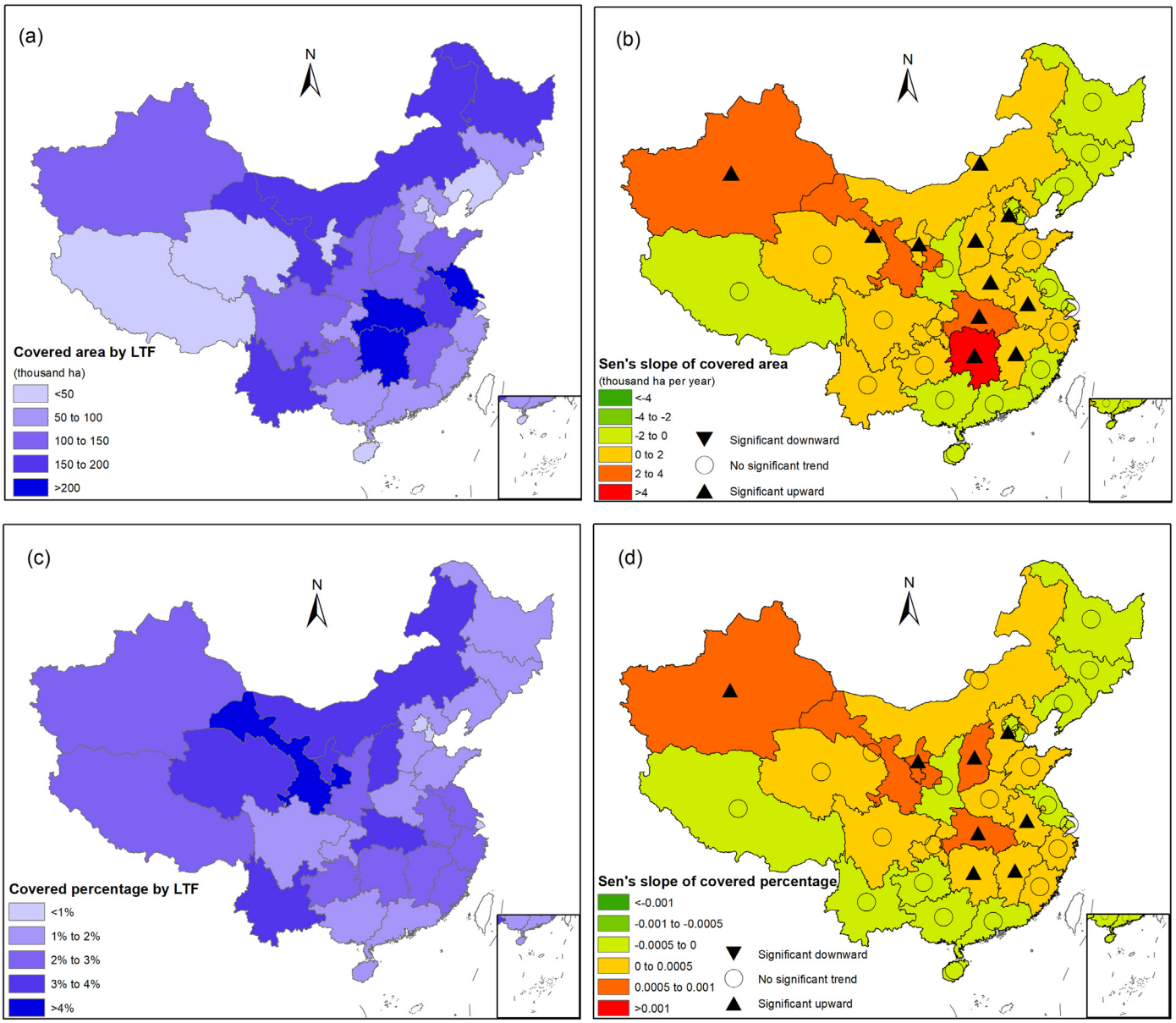

Fig. 7. Spatial distribution of covered area (a), covered percentage (c), and corresponding temporal change slope (b, d) from 1978 to 2018 by LTF.

11.4 million and 6.2 million ha per year. The yearly averaged covered area and affected area by hail and LTF were all smaller than 5 million ha. The changing trends in covered area and affected area by drought, flood, and hail disasters all showed decreasing trends, while only LTF showed an increasing trend with an extremely large value in 2008.

For the total covered and affected percentages by the four AMDs, relatively larger values were displayed in the northern part of China than in the southern part, suggesting that provinces in North China have a higher probability of being covered or affected by AMDs, that is, they have a higher vulnerability to AMDs induced by harsh natural agricultural conditions. Specific to the components of the total covered area and the components of the four different AMDs, more than 70% of covered area by AMDs were composed of drought and flooding, the two main disasters during 1978–2018 in most provincial districts. In all provincial districts of northern China, more than 50% of the covered area was induced by drought. In most provincial districts of southern China, more than 40% of the covered areas were induced by floods.

The covered area by drought in Inner Mongolia, Heilongjiang, Hebei, Shanxi, and Henan were relatively large exceeding 1.2 million ha, and the probability of being covered by drought has decreased in most parts of China. Cropland damage caused by flood disasters was mainly distributed in the middle to lower reaches of the Yangtze River basin, Songhua River basin, and Peral River basin. The significant increasing trends of the affected percentage observed in the middle Yangtze River basin demonstrated the need for implementing anti-flood agricultural measures. Hail disaster problems were prominent in Xinjiang, with a significant increasing trend among all parameters by hail. Compared with the other three AMDs, LTF covered and affected the smallest values of cropland area with the largest covered area value of around 0.2 million ha in southern provinces such as Hubei, Hunan, and Jiangsu. The results of this study systematically display the characteristics of four AMDs and their influence on cropland losses, which are critical and necessary for disaster risk reduction and adaptive strategy development.

CRediT authorship contribution statement

Ximeng Xu: Data curation, Formal analysis, Methodology, Visualization, Writing – original draft. **Qiuhong Tang:** Conceptualization, Funding acquisition, Writing – review & editing.

Declaration of competing interest

The authors declare that they have no known competing financial interests or personal relationships that could have appeared to influence the work reported in this paper.

Acknowledgement

This study is supported by the National Natural Science Foundation of China (41790424, 41730645, 41907060), Strategic Priority Research Program of Chinese Academy of Sciences (XDA20060402, XDA23100401).

Appendix A. Supplementary data

Supplementary data to this article can be found online at https://doi.org/10.1016/j.scitotenv.2021.147247.

References

Alcántara-Ayala, I., 2002. Geomorphology, natural hazards, vulnerability and prevention of natural disasters in developing countries. Geomorphology 47 (2–4), 107–124. https://doi.org/10.1016/S0169-555X(02)00083-1.

Chen, Y., Wang, K., Lin, Y., Shi, W., Song, Y., He, X., 2015. Balancing green and grain trade. Nat. Geosci. 8 (10), 739–741. https://doi.org/10.1038/nego2544.

Chen, X., Zhang, H., Chen, W., Huang, G., 2020. Urbanization and climate change impacts on future flood risk in the Pearl River Delta under shared socioeconomic pathways. Sci. Total Environ., 143144 https://doi.org/10.1016/j.scitotenv.2020.143144.

Chou, J., Xian, T., Zhao, R., Xu, Y., Yang, F., Sun, M., 2019. Drought risk assessment and estimation in vulnerable eco-regions of China: under the background of climate change. Sustainability 11 (16), 4463. https://doi.org/10.3390/su11164463.

Crompton, R.P., John McAneney, K., 2008. Normalised Australian insured losses from meteorological hazards: 1967–2006. Environ. Sci. Pol. 11 (5), 371–378. https://doi.org/10.1016/j.envsci.2008.01.005.

Dawood, M., 2017. Spatio-statistical analysis of temperature fluctuation using Mann–Kendall and Sen's slope approach. Clim. Dyn. 48 (3–4), 783–797. https://doi.org/10.1007/s00382-016-3110-y.

Fang, S.B., Yang, J.J., Zhou, G.S., 2011. Change trend and distributive characteristics of agrometeorological disasters in China in recent 30 years. J. Nat. Disasters 20 (5), 69–73 doi: CNKI:SUN:ZRZH.0.2011-05-010. (In Chinese).

Fang, J., Lincke, D., Brown, S., Nicholls, R.J., Wolff, C., Merkens, J.L., Hinkel, J., Vafeudus, A.T., Shi, P.J., Liu, M., 2020. Coastal flood risks in China through the 21st century–an application of DIVA. Sci. Total Environ. 704, 135311. https://doi.org/10.1016/j.scitotenv.2019.135311.

Feng, Z., Yang, Y., Zhang, Y., Zhang, P., Li, Y., 2005. Grain-for-green policy and its impacts on grain supply in West China. Land Use Policy 22 (4), 301–312. https://doi.org/10.1016/j.landusepol.2004.05.004.

Food and Agriculture Organization of the United Nations, 2018. The impact of disasters and crises on agriculture and food security 2017. http://www.fao.org/3/I8656EN/i8656en.pdf.

Fu, Q., Zhou, Z., Li, T., Liu, D., Hou, R., Cui, S., Yan, P., 2018. Spatiotemporal characteristics of droughts and floods in northeastern China and their impacts on agriculture. Stoch. Env. Res. Risk A. 32 (10), 2913–2931. https://doi.org/10.1007/s00477-018-1543-z.

Gao, J., 2016. Analysis and assessment of the risk of snow and freezing disaster in China. Int. J. Disaster Risk Reduction 19, 334–340. https://doi.org/10.1016/j.ijdrr.2016.09.007.

Gong, L., Hou, S., Su, B., Miao, K., Zhang, N., Liao, W., Zhong, S., Wang, Z., Yang, L., Huang, C., 2019. Short-term effects of moderate and severe floods on infectious diarrheal diseases in Anhui Province, China. Sci. Total Environ. 675, 420–428. https://doi.org/10.1016/j.scitotenv.2019.04.248.

Guan, Y., Zheng, F., Zhang, P., Qin, C., 2015. Spatial and temporal changes of meteorological disasters in China during 1950–2013. Nat. Hazards 75 (3), 2607–2623. https://doi.org/10.1007/s11069-014-1446-3.

Guo, J., Mao, K., Zhao, Y., Lu, Z., Lu, X., 2019. Impact of climate on food security in mainland China: a new perspective based on characteristics of major agricultural natural disasters and grain loss. Sustainability 11 (3), 869. https://doi.org/10.3390/su11030869.

Guo, J., Wu, X., Wei, G., 2020. A new economic loss assessment system for urban severe rainfall and flooding disasters based on big data fusion. Environ. Res. 188, 109822. https://doi.org/10.1016/j.envres.2020.109822.

Hamed, K.H., Ramachandra, R.A., 1998. A modified Mann–Kendall trend test for autocorrelated data. J. Hydrol. 204 (1), 182–196. https://doi.org/10.1016/S0022-1694(97)00125-X.

Hao, L., Zhang, X., Liu, S., 2012. Risk assessment to China's agricultural drought disaster in county unit. Nat. Hazards 61 (2), 785–801. https://doi.org/10.1007/s11069-011-0066-4.

He, B., Wu, J., Lv, A., Cui, X., Zhou, L., Liu, M., Zhao, L., 2013. Quantitative assessment and spatial characteristic analysis of agricultural drought risk in China. Nat. Hazards 66, 155–166. https://doi.org/10.1007/s11069-012-0398-8.

He, J., Yang, X., Li, Z., Zhang, X., Tang, Q., 2016. Spatiotemporal variations of meteorological droughts in China during 1961–2014: an investigation based on multi-threshold identification. Int. J. Disaster Risk Sci. 7 (1), 63–76. https://doi.org/10.1007/s13753-016-0083-8.

Huang, J., Lei, Y., Zhang, F., Hu, Z., 2017. Spatio-temporal analysis of meteorological disasters affecting rice, using multi-indices, in Jiangsu province, Southeast China. Food Secur. 9 (4), 661–672. https://doi.org/10.1007/s12571-017-0689-8.

Huang, J., Zhou, L., Zhang, F., Hu, Z., 2019. Quantifying the effect of temporal variability of agro-meteorological disasters on winter oilseed rape yield: a case study in Jiangsu province, southeast China. Environ. Monit. Assess. 191 (5), 276. https://doi.org/10.1007/s10661-019-7406-3.

Hui, G., 2009. China's snow disaster in 2008, who is the principal player? Int. J. Climatol. 29 (14), 2191–2196. https://doi.org/10.1002/joc.1859.

Intergovernmental Panel on Climate Change, 2012. Managing the Risks of Extreme Events and Disasters to Advance Climate Change Adaptation. A Special Report of Working Groups I and II of the Intergovernmental Panel on Climate Change. Cambridge University Press, Cambridge, UK, and New York, NY, USA https://www.ipcc.ch/report/managing-the-risks-of-extreme-events-and-disasters-to-advance-climate-change-adaptation/.

Intergovernmental Panel on Climate Change, 2019. Climate Change and Land, an IPCC Special Report on Climate Change, Desertification, Land Degradation, Sustainable Land Management, Food Security, and Greenhouse Gas Fluxes in Terrestrial Ecosystems. IPCC, Geneva, Switzerland https://www.ipcc.ch/srccl/.

Jin, J., Wang, W., Wang, X., 2016. Farmers' risk preferences and agricultural weather index insurance uptake in rural China. Int. J. Disaster Risk Sci. 7 (4), 366–373. https://doi.org/10.1007/s13753-016-0108-3.

Kendall, M.G., 1975. Rank Correlation Measures. Charles Griffin, London.

Kenyon, W., Hill, G., Shannon, P., 2008. Scoping the role of agriculture in sustainable flood management. Land Use Policy 25 (3), 351–360. https://doi.org/10.1016/j.landusepol.2007.09.003.

Kim, Y., Lee, S., 2019. Trends of extreme cold events in the central regions of Korea and their influence on the heating energy demand. Weather Clim. Extremes 24, 100199. https://doi.org/10.1016/j.wace.2019.100199.

Klomp, J., 2016. Economic development and natural disasters: a satellite data analysis. Glob. Environ. Chang. 36, 67–88. https://doi.org/10.1016/j.gloenvcha.2015.11.001.

Konisky, D.M., Hughes, L., Kaylor, C.H., 2016. Extreme weather events and climate change concern. Clim. Chang. 134 (4), 533–547. https://doi.org/10.1007/s10584-015-1555-3.

Li, Y., Ye, T., Liu, W., Gao, Y., 2018. Linking livestock snow disaster mortality and environmental stressors in the Qinghai-Tibetan Plateau: quantification based on generalized additive models. Sci. Total Environ. 625, 87–95. https://doi.org/10.1016/j.scitotenv.2017.12.230.

Liu, T., Yan, T.C., 2011. Main meteorological disasters in China and their economic losses. J. Nat. Disasters 20 (2), 90–95 (In Chinese).

Liu, Y., You, M., Zhu, J., Wang, F., Ran, R., 2019. Integrated risk assessment for agricultural drought and flood disasters based on entropy information diffusion theory in the middle and lower reaches of the Yangtze River, China. Int. J. Disaster Risk Reduction 38, 101194. https://doi.org/10.1016/j.ijdrr.2019.101194.

Mann, H.B., 1945. Non-parametric tests against trend. Econometrica. 13, 245–259. https://doi.org/10.2307/1907187.

National Bureau of Statistics of China, 2018. Chinese Statistical Yearbook. China Statistics Press, Beijing.

Parisse, B., Pontrandolfi, A., Epifani, C., Alilla, R., De Natale, F., 2020. An agrometeorological analysis of weather extremes supporting decisions for the agricultural policies in Italy. Ital. J. Agrometeorol. 1, 15–30. https://doi.org/10.13128/ijam-790.

Piao, S.L., Ciais, P., Huang, Y., et al., 2010. The impacts of climate change on water resources and agriculture in China. Nature 467, 43–50. https://doi.org/10.1038/nature09364.

Prein, A.F., Holland, G.J., 2018. Global estimates of damaging hail hazard. Weather Clim. Extremes 22, 10–23. https://doi.org/10.1016/j.wace.2018.10.004.

Qin, D.H., 2007. Major meteorological disasters impacting on China and their development situation. J. Nat. Disasters 16(z1, 46–48. https://doi.org/10.3969/j.issn.1004-4574.2007.z1.013 (in Chinese).

Qiu, X., Yang, X., Fang, Y., Xu, Y., Zhu, F., 2018. Impacts of snow disaster on rural livelihoods in southern Tibet-Qinghai Plateau. Int. J. Disaster Risk Reduction 31, 143–152. https://doi.org/10.1016/j.ijdrr.2018.05.007.

Roxburgh, N., Guan, D., Shin, K.J., Rand, W., Managi, S., Lovelace, R., Meng, J., 2019. Characterising climate change discourse on social media during extreme weather events. Glob. Environ. Chang. 54, 50–60. https://doi.org/10.1016/j.gloenvcha.2018.11.004.

Sen, P.K., 1968. Estimates of the regression coefficient based on Kendall's tau. J. Am. Stat. Assoc. 63 (324), 1379–1389. https://doi.org/10.1080/01621459.1968.10480934.

Shi, P.J., Ying, Z.R., 2016. Impact of meteorological disaster on economic growth in China. J. Beijing Normal Univ. Nat. Sci. 52 (6), 747–753 (in Chinese).

Shi, L., Zhao, P., Wang, X., 2015. Temporal and spatial distribution features of hail disaster in Xinjiang from 1961 to 2014. J. Glaciol. Geocryol. 37 (4), 898–904 (In Chinese).

Shi, W., Wang, M., Liu, Y., 2021. Crop yield and production responses to climate disasters in China. Sci. Total Environ. 750, 141147. https://doi.org/10.1016/j.scitotenv.2020.141147.

Shiru, M.S., Shahid, S., Chung, E.S., Alias, N., 2019. Changing characteristics of meteorological droughts in Nigeria during 1901–2010. Atmos. Res. 223, 60–73. https://doi.org/10.1016/j.atmosres.2019.03.010.

Sisco, M.R., Bosetti, V., Weber, E.U., 2017. When do extreme weather events generate attention to climate change? Clim. Chang. 143 (1–2), 227–241. https://doi.org/10.1007/s10584-017-1984-2.

Song, X., Song, S., Sun, W., Mu, X., Wang, S., Li, J., Li, Y., 2015. Recent changes in extreme precipitation and drought over the Songhua River Basin, China, during 1960–2013. Atmos. Res. 157, 137–152. https://doi.org/10.1016/j.atmosres.2015.01.022.

Stott, P., 2016. How climate change affects extreme weather events. Science 352 (6293), 1517–1518. https://doi.org/10.1126/science.aaf7271.
Su, W., Zhang, X.D., Wang, Z., Su, X.H., Huang, J.X., Yang, S.Q., Liu, S.C., 2011. Analyzing disaster-forming environments and the spatial distribution of flood disasters and snow disasters that occurred in China from1949 to 2000. Math. Comput. Model. 54 (3–4), 1069–1078. https://doi.org/10.1016/j.mcm.2010.11.037.
Sun, F., Mejia, A., Zeng, P., Che, Y., 2019. Projecting meteorological, hydrological and agricultural droughts for the Yangtze River basin. Sci. Total Environ. 696, 134076. https://doi.org/10.1016/j.scitotenv.2019.134076.
Tabari, H., Talaee, P.H., 2011. Analysis of trends in temperature data in arid and semi-arid regions of Iran. Glob. Planet. Chang. 79 (1–2), 1–10. https://doi.org/10.1016/j.gloplacha.2011.07.008.
Tang, Q., 2020. Global change hydrology: terrestrial water cycle and global change. Sci. China Earth Sci. 63, 459–462. https://doi.org/10.1007/s11430-019-9559-9.
Tang, Q., Zhang, X., Yang, X., Francis, J.A., 2013. Cold winter extremes in northern continents linked to Arctic sea ice loss. Environ. Res. Lett. 8 (1), 014036. https://doi.org/10.1088/1748-9326/8/1/014036.
Tang, R., Wu, J., Ye, M., Liu, W., 2019. Impact of economic development levels and disaster types on the short-term macroeconomic consequences of natural hazard-induced disasters in China. Int. J. Disaster Risk Reduction 10 (3), 371–385. https://doi.org/10.1007/s13753-019-00234-0.
The Ministry of Agriculture of the People"s Republic of China, 2018. China Agriculture Statistical Report. China Agriculture Press, Beijing.
The Ministry of Water Resources of the People"s Republic of China, 2018. Bulletin of Flood and Drought Disasters in China. China WaterPower Press, Beijing.
Von Storch, V.H., 1995. Misuses of statistical analysis in climate research. In: von Storch, H., Navarra, A. (Eds.), Analysis of Climate Variability: Applications of Statistical Techniques. Springer-Verlag, Berlin, pp. 11–26.
Wang, Y., Zhou, L., 2005. Observed trends in extreme precipitation events in China during 1961–2001 and the associated changes in large-scale circulation. Geophys. Res. Lett. 32 (9), L09707. https://doi.org/10.1029/2005GL022574.
Wang, J.A., Shi, P.J., Wang, P., et al., 2006. Temporal and Spatial Pattern of Natural Disasters in China. Science Press, Beijing.
Wang, Y., Zhang, Q., Wang, S.P., Wang, J.S., Yao, Y.B., 2017. Characteristics of agro-meteorological disasters and their risk in Gansu Province against the background of climate change. Nat. Hazards 89 (2), 899–921. https://doi.org/10.1007/s11069-017-2999-8.
Wang, Q., Liu, Y.Y., Zhang, Y.Z., Tong, L.J., Li, X., Li, J.L., Sun, Z., 2019a. Assessment of spatial agglomeration of agricultural drought disaster in China from 1978 to 2016. Sci. Rep. 9 (1), 1–8. https://doi.org/10.1038/s41598-019-51042-x.
Wang, Y., Liu, G., Guo, E., 2019b. Spatial distribution and temporal variation of drought in Inner Mongolia during 1901–2014 using Standardized Precipitation Evapotranspiration Index. Sci. Total Environ. 654, 850–862. https://doi.org/10.1016/j.scitotenv.2018.10.425.
World Meteorological Organization, 2020. WMO Statement on the State of the Global Climate in 2019. World Meteorological Organization, p. 29. https://public.wmo.int/en/resources/library/wmo-statement-state-of-global-climate-2019.
Wu, J.D., Fu, Y., Zhang, J., Li, N., 2014. Meteorological disaster trend analysis in China: 1949–2013. J. Nat. Res. 29 (9), 1520–1530. https://doi.org/10.11849/zrzyxb.2014.09.007 (in Chinese).
Wu, M., Chen, Y., Wang, H., Sun, G., 2015. Characteristics of meteorological disasters and their impacts on the agricultural ecosystems in the northwest of China: a case study in Xinjiang. Geoenviron. Disasters 2 (1), 3. https://doi.org/10.1186/s40677-015-0015-8.
Wu, J., Huang, C., Pang, M., Wang, Z., Yang, L., FitzGerald, G., Zhong, S., 2019. Planned sheltering as an adaptation strategy to climate change: lessons learned from the severe flooding in Anhui Province of China in 2016. Sci. Total Environ. 694, 133586. https://doi.org/10.1016/j.scitotenv.2019.133586.
Wu, X., Wang, Z., Gao, G., Guo, J., Xue, P., 2020. Disaster probability, optimal government expenditure for disaster prevention and mitigation, and expected economic growth. Sci. Total Environ. 709, 135888. https://doi.org/10.1016/j.scitotenv.2019.135888.
Xu, L., Zhang, Q., Zhang, J., Zhao, L., Sun, W., Jin, Y., 2017. Extreme meteorological disaster effects on grain production in Jilin Province, China. J. Integr. Agric. 16 (2), 486–496. https://doi.org/10.1016/S2095-3119(15)61285-0.
Yan, T.W., Zhang, T.C., Zhang, J.B., 2017. Research on natural disaster vulnerability and its poverty-causing effect in contiguous poor rural areas. Chin. J. Agrometeorol. 38, 526–536. https://doi.org/10.3969/j.issn.1000-6362.2017.08.007.
Yang, M., Mou, Y., Meng, Y., Liu, S., Peng, C., Zhou, X., 2020. Modeling the effects of precipitation and temperature patterns on agricultural drought in China from 1949 to 2015. Sci. Total Environ. 711, 135139. https://doi.org/10.1016/j.scitotenv.2019.135139.
Yao, Y.Q., Zheng, F.L., Guan, Y.H., 2017. The temporal and spatial characteristics of flood and drought during the recent 60 years in China. Agric. Res. Arid Areas. 35 (1), 228–232. https://doi.org/10.7606/j.issn.1000-7601.2017.01.34 (in Chinese).
Yao, N., Li, L., Feng, P., Feng, H., Li, Y., 2020. Projections of drought characteristics in China based on a standardized precipitation and evapotranspiration index and multiple GCMs. Sci. Total Environ. 704, 135245. https://doi.org/10.1016/j.scitotenv.2019.135245.
Ye, T., Liu, W., Mu, Q., Zong, S., Li, Y., Shi, P., 2020. Quantifying livestock vulnerability to snow disasters in the Tibetan Plateau: comparing different modeling techniques for prediction. Int. J. Disaster Risk Reduction 48, 101578. https://doi.org/10.1016/j.ijdrr.2020.101578.
Yin, Y.X., Xu, Y.P., Chen, Y., 2009. Relationship between flood/drought disasters and ENSO from 1857 to 2003 in the Taihu Lake basin, China. Quat. Int. 208 (1–2), 93–101. https://doi.org/10.1016/j.quaint.2008.12.016.
You, Q., Kang, S.C., Aguilar, E., Pepin, N., Flugel, W., Yan, Y., Xu, Y., Zhang, Y., Huang, J., 2011. Changes in daily climate extremes in China and their connection to the large scale atmospheric circulation during 1961–2003. Clim. Dyn. 36 (11−12), 2399–2417. https://doi.org/10.1007/s00382-009-0735-0.
Yue, S., Wang, C.Y., 2002. Applicability of prewhitening to eliminate the influence of serial correlation on the Mann-Kendall test. Water Resour. Res. 38 (6), 1–7. https://doi.org/10.1029/2001WR000861.
Yue, S., Pilon, P., Phinney, B., Cavadias, G., 2002. The influence of autocorrelation on the ability to detect trend in hydrological series. Hydrol. Process. 16, 1807–1829. https://doi.org/10.1002/hyp.1095.
Zhang, J.Q., 2004. Risk assessment of drought disaster in the maize-growing region of Songliao Plain, China. Agric. Ecosyst. Environ. 102 (2), 133–153. https://doi.org/10.1016/j.agee.2003.08.003.
Zhang, Z., Wang, P., Chen, Y., Zhang, S., Tao, F.L., Liu, X.F., 2014a. Spatial pattern and decadal change of agro-meteorological disasters in the main wheat production area of China during 1991–2009. J. Geogr. Sci. 24 (3), 387–396. https://doi.org/10.1007/s11442-014-1095-1.
Zhang, Z., Chen, Y., Wang, P., Zhang, S., Tao, F.L., Liu, X.F., 2014b. Spatial and temporal changes of agro-meteorological disasters affecting maize production in China since 1990. Nat. Hazards 71 (3), 2087–2100. https://doi.org/10.1007/s11069-013-0998-y.
Zhou, Y., Li, N., Wu, W., Liu, H., Wang, L., Liu, G., Wu, J., 2014. Socioeconomic development and the impact of natural disasters: some empirical evidences from China. Nat. Hazards 74 (2), 541–554. https://doi.org/10.1007/s11069-014-1198-0.
Zhou, Y., Liu, Y., Wu, W., Li, N., 2015. Integrated risk assessment of multi-hazards in China. Nat. Hazards 78 (1), 257–280. https://doi.org/10.1007/s11069-015-1713-y.
Zhou, L., Wu, J., Mo, X., Zhou, H., Diao, C., Wang, Q., Chen, Y., Zhang, F., 2017. Quantitative and detailed spatiotemporal patterns of drought in China during 2001–2013. Sci. Total Environ. 589, 136–145. https://doi.org/10.1016/j.scitotenv.2017.02.202.